

**Mitochondria-derived peptide SHLP2 regulates energy homeostasis through the
activation of hypothalamic neurons**

Seul Ki Kim^{1,2}, Le Trung Tran^{1,2}, Cherl NamKoong³, Hyung Jin Choi^{3,4}, Hye Jin Chun⁵,
Yong-ho Lee⁵, MyungHyun Cheon⁶, ChiHye Chung⁶, Junmo Hwang⁷, Hyun-Ho Lim⁷, Dong
Min Shin^{1,2}, Yun-Hee Choi¹, and Ki Woo Kim^{1,2*}

¹Division of Physiology, Department of Oral Biology, Yonsei University College of Dentistry,
Seoul, 03722, Korea

²Department of Applied Life Science, BK21 FOUR, Yonsei University College of Dentistry,
Seoul, 03722, Korea

³Neuroscience Research Institute, Seoul National University College of Medicine, Seoul,
03080, Korea

⁴Department of Biomedical Sciences, Seoul National University College of Medicine, Seoul,
03080, Korea

⁵Department of Internal Medicine, Yonsei University College of Medicine, Seoul, 03722,
Korea

⁶Department of Biological Sciences, Konkuk University, Seoul, 05029, Korea

⁷Neurovascular Unit Research Group, Korea Brain Research Institute (KBRI), Daegu, 41068,
Korea

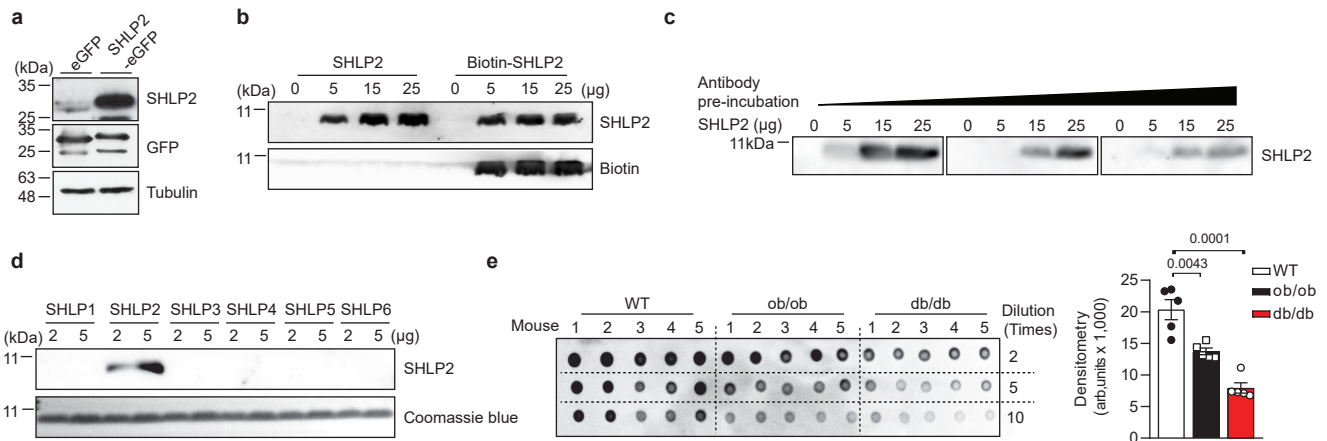
*Correspondence and reprints, materials should be addressed to:

Ki Woo Kim (kiwoo-kim@yuhs.ac)

SUPPLEMENTARY INFORMATION

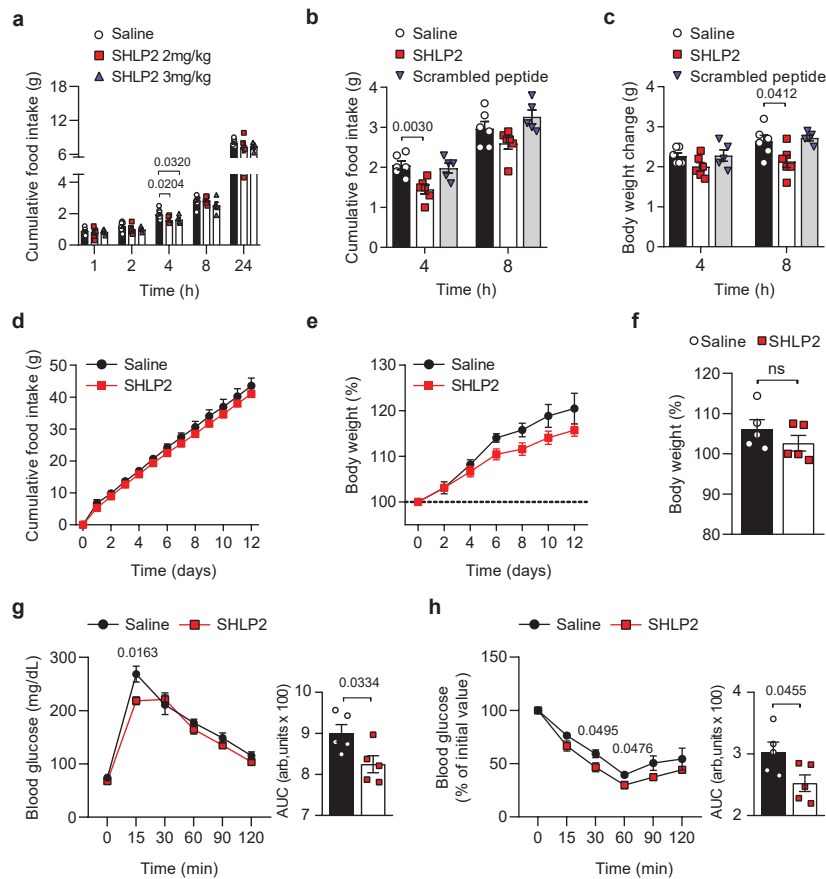
Supplementary Figure 1-6

Supplementary Tables 1-3



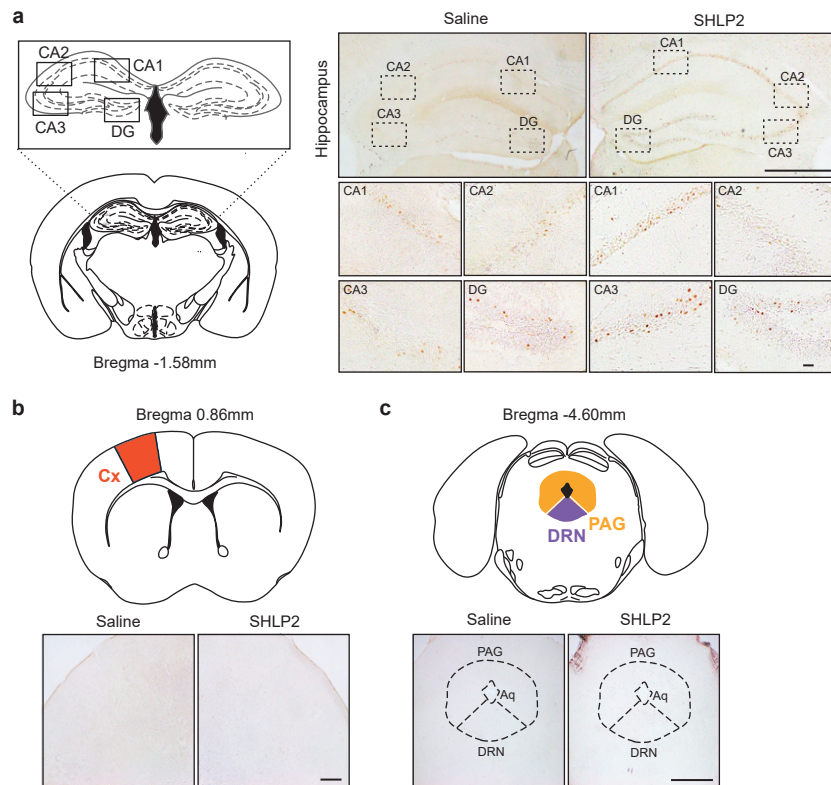
Supplementary Fig. 1: Validation of SHLP2 antibody.

a, Detection of SHLP2 after overexpression of SHLP2-eGFP construction in HEK 293 cells. Western blots were performed using anti-SHLP2, anti-GFP or anti-tubulin antibodies. **b**, Detection of SHLP2 and biotinylated SHLP2 peptides using anti-SHLP2 and anti-biotin antibodies. **c**, Peptide competition assays using SHLP2 peptides. Anti-SHLP2 antibody was incubated in the presence of increasing amounts (1, 5, 15, 25 μg) of each peptide indicated. **d**, Detection of SHLP1 to 6 using anti-SHLP2 antibody. **e**, Dot-blot image (left) and relative blot densitometry (right) detecting plasma SHLP2 levels in WT, *ob/ob* and *db/db* male mice ($n = 5$ each group). Data shown are representative of three independent experiments with similar results (**a-d**). n indicates the number of biologically independent mice examined. Data were presented as mean \pm SEM. Two-tailed Student's t-tests were used. Source data are provided as a Source Data file.



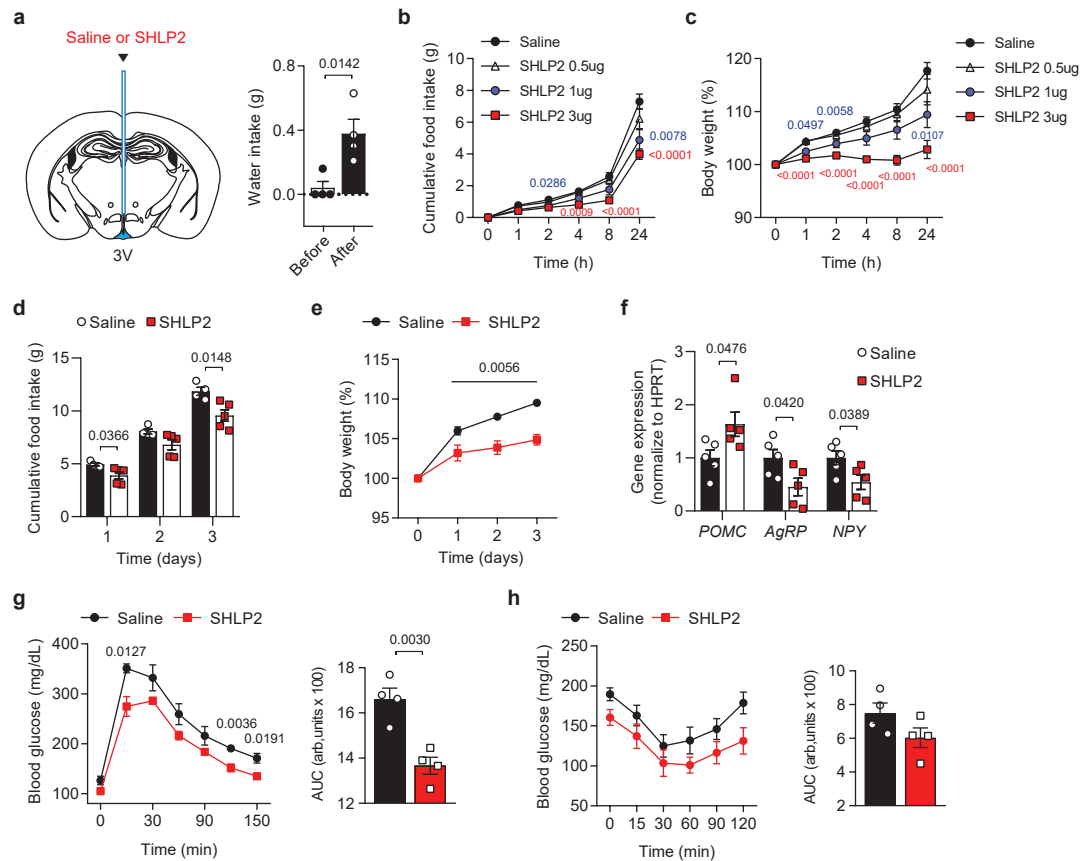
Supplementary Fig. 2: Temporal changes in food intake and body weight, as well as the results of the ITT and GTT, in normal chow-fed mice after an IP injection of SHLP2

a, Cumulative food intake (left) of male mice fed with NC after IP injection of saline or 2, 3mg/kg SHLP2 ($n = 9$ saline, $n = 5$ each SHLP2 group). **b-c**, Cumulative food intake (**b**) and body weight change (**c**) of male mice fed with NC after IP injection of saline or SHLP2 or scrambled peptide following an overnight fasting ($n = 6$ saline, $n = 6$ SHLP2, $n = 5$ scrambled peptide). **d-e**, Cumulative food intake (**d**) and body weight change (% of initial) (**e**) were monitored after daily IP injection of either saline or SHLP2 in male mice ($n = 3$ saline, $n = 5$ SHLP2). **f**, Body weight (% of initial) of male mice fed with NC after daily IP injection of saline or SHLP2 for 3 weeks ($n = 5$ each group). **g-h**, GTT (**g**) and ITT (**h**) were performed in NC-fed male mice after 3 weeks of IP administration of saline or SHLP2 ($n = 5$ each group). n indicates the number of biologically independent mice examined. Data were presented as mean \pm SEM. Two-tailed Student's t-tests were used. Source data are provided as a Source Data file.



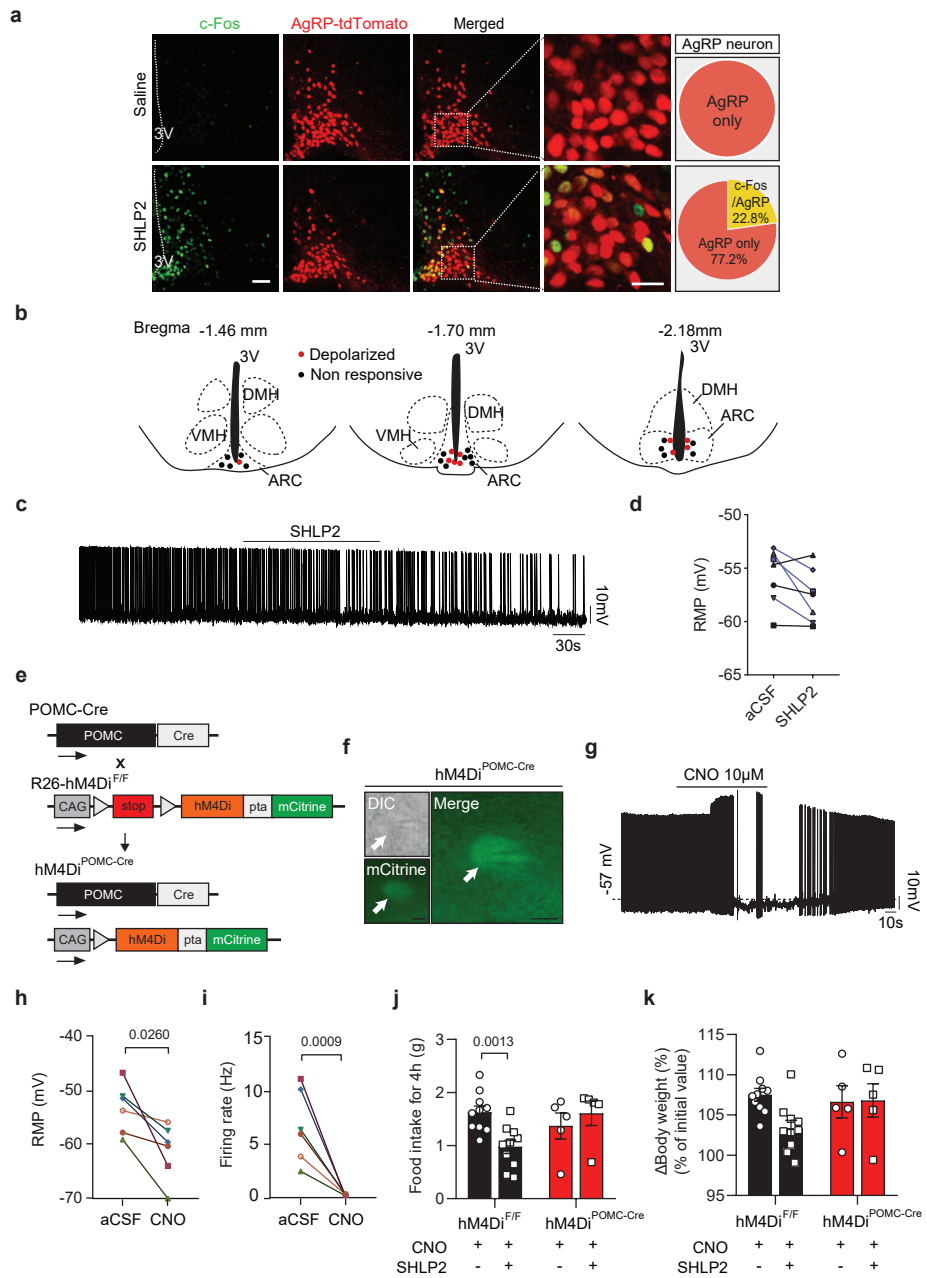
Supplementary Fig. 3: c-Fos activation in different brain regions in response to SHLP2.

a-c, c-Fos immunoactivity after SHLP2 administration (IP) in the hippocampus (**a**), cortex (Cx, **b**), periaqueductal gray (PAG, **c**) and dorsal raphe nucleus (DRN, **c**) ($n = 4$ each group). CA, cornu amonis. DG, dentate gyrus. Aq, aqueduct. n indicates the number of biologically independent mice examined. Scale bars, 100 μ m. Source data are provided as a Source Data file.



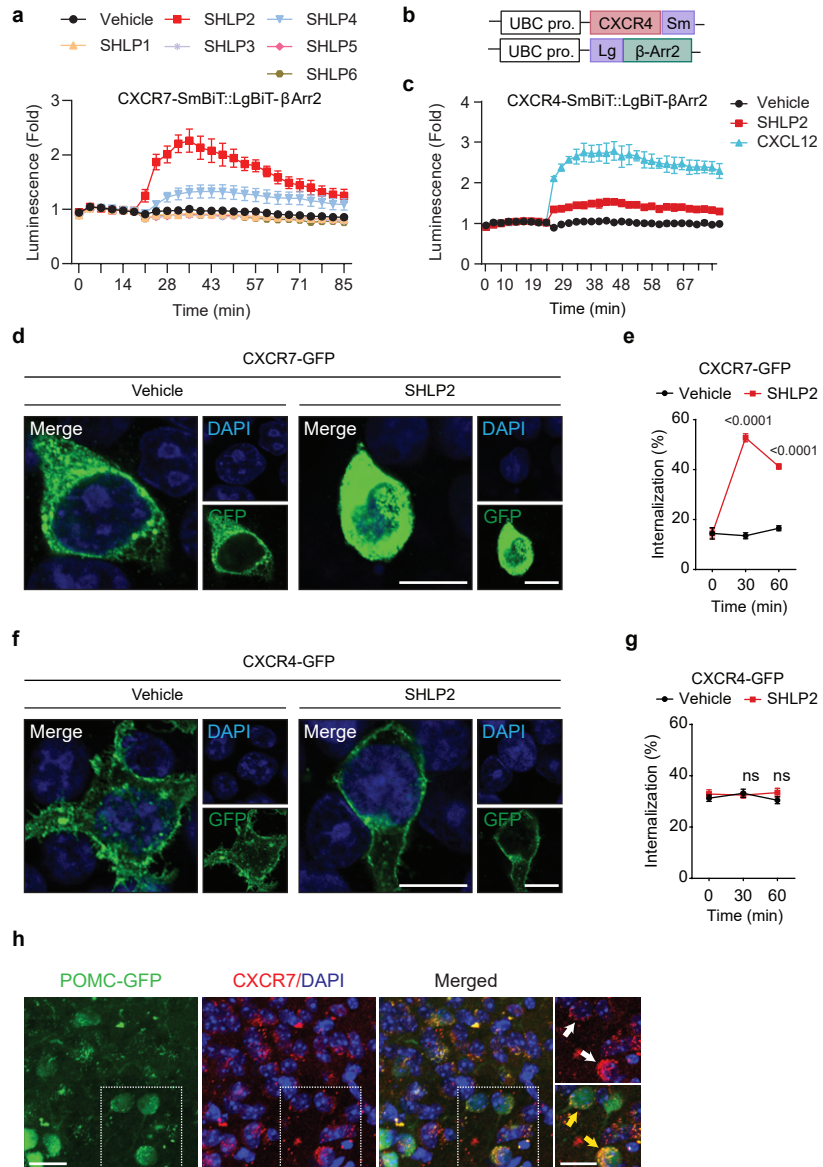
Supplementary Fig. 4: Long-term SHLP2 treatment ameliorates HFD-induced obesity.

a, Schematic for experimental configuration. A guide cannula was implanted to the 3V to deliver saline or SHLP2 (left). Water intake (right) following an acute ICV administration of angiotensin II ($n = 4$ each group). **b-c**, Cumulative food intake (**b**) and body weight (% of initial) (**c**) of male mice fed with NC after ICV injection of saline or 0.5, 1, 3 μ g SHLP2 ($n = 10$ each group). **d-e**, Cumulative food intake (**d**) and body weight (% of initial) (**e**) of HFD-fed male mice following a single ICV injection of saline or SHLP2 ($n = 4$ saline, $n = 5$ SHLP2). **f**, The *Pomc*, *AgRP* and *Npy* expression in the hypothalamus of male mice fed HFD after one hour of ICV injection of Saline or SHLP2 ($n = 4$ saline, $n = 5$ SHLP2). **g-h**, GTT (**g**) and ITT (**h**) were performed in HFD-fed male mice after 4 hours of ICV administration of saline or SHLP2 ($n = 4$ each group). n indicates the number of biologically independent mice examined. Data were presented as mean \pm SEM. Two-tailed Student's t-tests were used, and two-way ANOVA with Bonferroni post-hoc tests were used in figure (**e**). Source data are provided as a Source Data file.



Supplementary Fig. 5: Effect of SHLP2 on POMC and AgRP neurons.

a, Percentage of c-Fos activation in AgRP neurons after an ICV administration of SHLP2 ($n = 3$). Scale bars, 20 μ m. **b**, Diagram showing the location and responses of recorded POMC neurons across the mediobasal hypothalamus. **c-d**, Representative trace (**c**) of AgRP neurons and effects on resting membrane potential (RMP) (**d**) of a subset of AgRP neurons. **e**, Schematic strategy for recombinant transgenes to generate hM4Di^{POMC-Cre} male mice. **f**, Fluorescent and DIC figures of targeted POMC neurons expressing the Cre-dependent modified form of the hM4Di receptor in fusion with the fluorescence protein mCitrine. The arrows indicate the targeted cell ($n = 6$ from 2 animals). **g-i**, Representative inhibition of POMC neuron (**g**) by CNO application. CNO induced hyperpolarization of POMC neurons expressing hM4Di, showing through decreases in the resting membrane potentials (**h**) and firing rates (**i**) ($n = 6$ from 2 animals). **j-k**, Cumulative food intake (**j**) and Δ body weight (%) (**k**) in hM4Di^{POMC-Cre} male mice after ICV SHLP2 administration with CNO injection ($n = 10$ each hM4Di^{F/F} group, $n = 5$ each hM4Di^{POMC-Cre} group). Scale bars, 5 μ m. n indicates the number of biologically independent mice examined. Data were presented as mean \pm SEM. Two-tailed Student's t-tests were used. Wilcoxon matched-pairs signed rank test were used in electrophysiological result. CAG, CMV immediate enhancer/ β -actin promoter; hM4Di, Gi-coupled hM4D DREADD; pta, porcine Teschovirus cleavage site; mCitrine; citrine fluorescence. Source data are provided as a Source Data file.



Supplementary Fig. 6: SHLP2 interacts specifically with CXCR7, but not CXCR4.

a, The β -Arrestin2 recruitment to CXCR7 by SHLP 1 to 6 ($n = 4$ each group). Note that the only SHLP2 exhibited specific activity. **b**, The DNA constructs used to for the NanoLuc complementation-based β -Arrestin2 recruitment to the chemokine receptor CXCR4. **c**, Representative result of β -Arrestin2 recruitment assay to CXCR4 ($n = 3$ saline, $n = 3$ CXCL12, $n = 4$ SHLP2). Note that there is no notable activity by SHLP2 **d**, Representative immunofluorescent staining of CXCR7 upon the application of SHLP2. **e**, The percentage of internalized receptors CXCR7 at different time points after the treatment of SHLP2 ($n = 3$ each group). **f**, Representative immunofluorescent staining of CXCR4 upon the application of SHLP2. **g**, The percentage of internalized receptors CXCR4 at different time points after the treatment of SHLP2 ($n = 3$ each group). Scale bars, $10\mu\text{m}$. **h**, Representative images of CXCR7 expression in POMC neurons ($n = 3$ each group). Scale bars, $50\mu\text{m}$. n indicates the number of biologically independent experimental groups examined. Data were presented as mean \pm SD. ns: no significance by two-way ANOVA followed by Sidak multiple comparison tests (**e and g**). Source data are provided as a Source Data file.

Supplementary Table 1. The clinical characteristics of the study subjects

	Healthy (n= 7)	Obese (n= 6)	Diabetic (n= 7)
Age (year)	55.1± 14.9	41.3±23.7	42.3± 18.7
BMI (kg/m ²)	22.6±5.1	31.9±2.9	31.4±2.3
TG (mg/dL)	85.4± 101.8	192.2± 164.8	174.4± 190.6
Cholesterol (mg/dL)	195.3±43.7	217.2±32.2	202.3±28.7
AST (U/L)	24.9±9.1	36.8±21.2	34.4± 18.6
ALT (IU/L)	22.7± 19.3	60.6±42.4	62.0±39
Gamma-GT (U/L)	14.7± 11.3	46.8±45.2	57.9±61.1

BMI, Body mass index; TG, Triglyceride; AST, Aspartate aminotransferase; ALT, Alanine aminotransferase; Gamma-GT, Gamma-glutamyl transferase

Supplementary Table 2. Primer sequences used for RT-PCR analyses

Gene	Forward primer (5' -3')	Reverse primer (5' -3')
<i>Ucp1</i>	GGCAACAAGAGCTGACAGTA	GGCCCTTGTAACAACAAAA
<i>Cox2</i>	ATAACCGAGTCGTTCTGCCAAT	TTTCAGAGCATTGGCCATAGAA
<i>Rps18</i>	TGTGTTAGGGGACTGGTGGACA	CATCACCCACTTACCCCAAAA
<i>Pomc</i>	CAGGTCCTGGAGTCCGAC	CATGAAGCCACCGTAACG
<i>Npy</i>	CTACTCCGCTCTGCGACACT	AGTGTCTCAGGGCTGGATCTC
<i>AgRP</i>	CGGCCACGAACCTCTGTAG	CTCATCCCCTGCCTTTGC
<i>Cart</i>	AGAAGAAGTACGGCCAAGTC	GGACAGTCACACAGCTTCC
<i>Pgc1α</i>	AACCACACCCACAGGATCAGA	TCTTCGCTTTATTGCTCCATGA
<i>Dio2</i>	TTCTCCAAGTGCCTCTTCCTG	CCCATCAGCGGTCTTCTCC
<i>Pparγ</i>	CAAGAATACCAAAGTGCATCAA	GAGCTGGTCTTTTCAGAATAAAG
<i>Srebp-1c</i>	GGAGCCATGGATTGCACATT	GGCCCGGGAAGTCACTGT
<i>Fasn</i>	GGTGTGGTGGGTTTGGTGAATTGT	TCACGAGTCATGCTTTAGCACCT
<i>Hprt</i>	CTCATGGACTGATTATGGACAGGAC	GCAGGTCAGCAAAGAACTTATAGCC
<i>Scd1</i>	AGTGCAGCAGGACCATGAGAATGA	TCCCTCCGAAATGAACGAGAGAA
<i>Acaca</i>	AGGAAGATGGTGTCCCGCTCTG	GGGAGATGTGCTGGGTCAT
<i>Fabp4</i>	AAGAGAAAACGAGATGGTGACAA	CTTGTGGAAGTCACGCCTTT
<i>Prdm16</i>	CGTCCACACGGAAGAGCGTGA	TGGAGTTGCTGGGGTCCGT
<i>Nrf1</i>	CGATGGGATTCCAGTCTCTGT	TGAGCATCTCTGGGATAAATGC

Supplementary Table 3. Sequences of peptides

Peptide name	Sequence
Small humanin-like peptide 1 (SHLP1)	MCHWAGGASNTGDARGDVFGKQAG
Small humanin-like peptide 2 (SHLP2)	MGVKFFTLSTRFFPSVQRAVPLWTNS
Small humanin-like peptide 3 (SHLP3)	MLGYNFSSFPCGTISIAPGFNFYRLYFIWVNGLAKVWW
Small humanin-like peptide 4 (SHLP4)	MLEVMFLVNRRGKICRVPFTFFNLSL
Small humanin-like peptide 5 (SHLP5)	MYCSEVGFCESEVAPTEIFNAGLVV
Small humanin-like peptide 6 (SHLP6)	MLDQDIPMVQPLLKVRLEND
Scrambled peptide	MKSFRVTVRPASLTSGVFTNLQFPWF